J Therm Anal Calorim (2014) 117:961–972
DOI 10.1007/s10973-014-3845-9

Combustion kinetics of two core materials for sandwich structures

Carmen Branca · Colomba Di Blasi

Received: 23 October 2013 / Accepted: 2 May 2014 / Published online: 28 May 2014

Abstract The thermal behavior of a polymeric foam (Divinycell H100) and balsa wood (ProBalsa LD7), which are extensively applied as core materials for sandwich panels, is investigated. Chars, produced from pyrolysis of thick samples at 950 K, reflect significant shrinkage of the sample and, for the polymeric foam, the complete loss of the cellular structure following softening. Thermogravimetric curves, measured in air at different heating rates, show that combustion takes place over a temperature range of 650–940 K (polymeric foam) and 475–740 K (balsa). The curves are well predicted by a four-step and a six-step reaction model, respectively, with kinetic parameters that are invariant with the heating rate.

Keywords Polymeric foam · Balsa wood · Combustion · Kinetics

Introduction

Sandwich structures are extensively applied in several industrial sectors. They consist of fiber-reinforced polymer skins laminated onto a light core made of polymeric foams, end-grain balsa wood, or aramid honeycomb [1]. This configuration provides both high specific strength and high specific stiffness but organic polymers are flammable. Thus, in addition to mechanical resistance, the thermal response and the combustion kinetics of the sandwich materials should be carefully examined as related data are also needed to develop transport models for the fire behavior of these multilayered structures [2–5]. The combustion characteristics of skin materials have also been investigated for composites of interest in practical applications [6, 7]. On the contrary, very little attention has been dedicated to core materials in these structures, in particular polymeric foams based on poly-vinyl-chloride (PVC) and balsa wood.

One of the cellular foams, based on PVC and most frequently used for the core of sandwich panels, bears the commercial name of Divinycell (for instance, see [8, 9]). The fundamental aspects of PVC thermal degradation are discussed in a comprehensive review [10]. Thermogravimetric curves in inert environments, which show mass loss over the temperature range of 473–793 K, have been used to construct kinetic models for the degradation [11–16]. The first step involves loss of HCl (and small quantities of hydrocarbons) to produce polyene, which then undergoes two competing degradation reactions to produce either volatiles or a cross-linked intermediate, which degrades at a higher temperature to produce more volatile materials and a stable char [14, 15]. However, the Divinycell foam also includes other chemical components which are expected to modify the decomposition reaction paths and products [17], not to mention that thermal degradation mechanisms do not take into account the effects of oxygen on solid devolatilization and exclude the combustion of the solid residue. In reality, the combustion behavior and the

C. Branca (✉)
Istituto di Ricerche sulla Combustione, C.N.R., P.le V. Tecchio, 80125 Naples, Italy
e-mail: branca@irc.cnr.it

C. Di Blasi
Dipartimento di Ingegneria Chimica, dei Materiali e della Produzione Industriale, Università degli Studi di Napoli "Federico II", P.le V. Tecchio, 80125 Naples, Italy

C. Di Blasi
IMAST— Distretto Tecnologico sull'Ingegneria dei Materiali Polimerici e Compositi e Strutture, P.zza Bovio 22, 80133 Naples, Italy

reaction kinetics for the Divinycell foam have never been examined.

The processes of wood thermal decomposition and combustion [18, 19] have been extensively studied in relation to both fire safety science and thermochemical conversion processes but, owing to the very specific uses, balsa wood has received very limited attention. Thanks to the very high permeability and the facility to absorb water, it has been used to mimic the combustion characteristics of watery waste materials, such as kitchen garbage [20]. The changes at a microscopic level [21] and in the thermal properties [22] during fire exposures of balsa coupons, as well as the fire performance of balsa sandwich panels [5, 23–25], have been examined. Moreover, thermogravimetric curves in nitrogen have been measured and interpreted by means of a one-step or a two-step model [22]. However, the solid-phase (char) combustion reactions are not considered and it cannot be excluded that the variability of the estimated parameters with the heating rate is indicative of possible compensation effects [26]. Moreover, the proposed mechanisms and the estimated parameter values (in particular the activation energies) are not in agreement with the current state of the art about the combustion kinetics of lignocellulosic materials (see the review [18] and the more recent survey on the problem background given in [27] with the formulation of a unified kinetic model).

This study examines the changes undergone by a polymeric foam (Divinycell H100) and balsa wood (ProBalsa LD7) when subjected to high-temperature pyrolysis. Also, thermogravimetric measurements are made in air of both materials and are used to formulate multi-step combustion models including the evaluation of the related kinetic parameters.

Materials and methods

Materials

The materials studied are a closed-cell polymeric foam, designed as Divinycell H100 (nominal density 100 kg m^{-3}), and end-grain (grain oriented along the thickness) balsa wood, designed as ProBalsa LD7 (nominal density 90 kg m^{-3}), both supplied by DIAB. The former belongs to a class of rigid polymeric foams made of alloys of PVC (30–75 %), aromatic polyurea (15–50 %), and polyamide (3–10 %) [28]. Balsa (Ochroma pyramidale) belongs to the hardwood family which typically consists of 43–46 % cellulose, 20–25 % lignin, 30–35 % hemicellulose, and small contents (1–5 %) of extractives [29]. Both materials are pre-dried with exposure in an oven at 373 K overnight, before the experimental tests.

Experimental

To investigate the thermogravimetric behavior of the two core materials in air, a system and a procedure, previously developed and extensively applied to study the conversion of condensed-phase fuels under conditions of kinetic control [6, 7, 30–35], are used. The combustion of the solid is made to occur under known thermal conditions with a proper control of the sample temperature (measured by a close-coupled thin thermocouple), using the intensity of the applied radiative heat flux as the adjustable variable. The characteristic size of the process is the thickness of the sample layer, whose limit value for a kinetic control depends on the nature of the solid fuel and the heating conditions. Similar to previous measurements made for lignocellulosic fuels, the balsa wood is reduced to powder (particles below 80 μm) and packed in layers about 110 μm thick (4 mg distributed over a surface 20 × 5 mm^2) which, for heating rates up to 20 K min^{-1} and a final temperature of 873 K, permit an excellent temperature control and avoid mass transport limitations (measurements are made for 5, 10, and 20 K min^{-1}). Conventional milling is found not to produce acceptable results for the Divinycell sample. Instead of searching alternative and more complicated milling procedures, the same approach successfully applied for a composite honeycomb material, which showed the same difficulties [36], is used. It consists of cutting thin material strips that are then subjected to thermogravimetric analysis. More specifically, strips with a surface of 1.8 × 5 mm^2 and a mass of 5.5 mg are prepared. A good temperature control and negligible heat and mass transfer limitations are achieved for samples showing these characteristics given heating rates up to 15 K min^{-1} and a final temperature of 950 K (measurements are made for heating rates of 5, 10, and 15 K min^{-1}). Each thermogravimetric test is made in triplicate, showing good repeatability (maximum deviations between the measured mass loss curves are always in the range of 0.1–0.3 %).

The thermogravimetric system is also used for a differential thermal analysis of the samples [34]. As a first step, the profile of the heat flux needed to heat the empty sample holder with an assigned rate from ambient to a final temperature is determined. Then the temperature of the sample is measured when subjected to the heat flux profile previously measured. The difference between the sample and the empty sample holder temperatures is used to provide indication about the energetics of the phase change and chemical reaction processes. The behavior of the two materials of interest is examined for a mass of 7 mg (samples prepared according to the procedures already described) and the empty sample holder temperature that

increases from ambient conditions up to 950 K with a rate of 15 K min^{-1}.

Pyrolysis experiments for thick samples, in the shape of parallelepiped with length 20 mm and width 15 × 15 mm^2, are also carried out, to investigate the morphological changes which the original materials undergo while producing char. The sample is instantaneously suspended, by means of a stainless steel mesh basket, in the isothermal zone of a cylindrical stainless reactor [6, 7, 29, 31], previously preheated at a temperature of 950 K. The temperature at the sample center is monitored by a 1-mm K thermocouple. Each test is again made in triplicate, showing an excellent reproducibility in relation to the char yield. The structure of the charred residues, collected at the conclusion of the tests, is studied by means of scanning electron microscope (SEM) images. Also, the chars produced are milled in particles of sizes below 80 μm and subjected to thermogravimetric analysis in air (3.5 mg distributed over a surface of 20 × 5 mm^2) for a heating rate of 5 K min^{-1} up to a final temperature of 950 K.

Results

In the first part of this section, the structure of the chars produced from pyrolysis of Divinycell and balsa is discussed. Then the main characteristics shown by the thermogravimetric curves are presented together with the formulation of multi-step combustion models and the estimation of the related kinetic constants.

Morphological structure of char

The thick samples are rapidly heated when exposed to the hot inert (nitrogen) environment, as testified by the relatively short time (60–90 s) required for the center to attain the reactor temperature of 950 K. Thermal degradation leads to charred residues corresponding to 42 mass % (Divinycell) and 19.5 mass % (balsa). The char yield obtained for the polymeric foam is significantly higher than the small values typically reported for the degradation of PVC [11, 12, 14, 15], although these increase significantly for the cross-linked samples [13]. The properties of PVC used for the polymeric foam under study are not known. Furthermore, the other two chemical components (aromatic polyurea and polyamide), which may also be present in significant quantities, can be partly responsible for the formation of char (for thermogravimetric conditions, these amount to about 20 % for polyureas [37] and around 10 % for polyamides [38]) and may modify the decomposition reaction paths and products of PVC (in particular polyamides [17]). Indeed the degradation of the three components of the polymeric foam takes place over overlapping temperature ranges (values typically reported are 473–793 K for PVC [11–16], 530–630 K for polyureas [37], and 750–870 K for polyamides [39]), thus enhancing their mutual interactions. On the other hand, the char yields produced from balsa are those typically obtained from thick wood samples at high temperatures [39, 40].

At a first glance from the snapshot reported in Fig. 1a, it appears that the polymeric foam shrinks and completely loses its shape/structure with the charred residue manifesting the passage through softening and partial melting. As a consequence of thermal degradation, important morphological changes occur at the microscopic level. These can be observed by means of the SEM images found in Fig. 2a–d which compare the structure of the original, un-reacted material (Fig. 2a–b), and the corresponding charred one (Fig. 2c–d). As already observed in [9], the microstructure of the un-reacted material comprises closed-cells, with an average cell size of about 350 micron (Fig. 2a–b).The cellular structure is completely absent from the charred residue (Fig. 2c), where the passage through a partially molten-phase during the degradation process is evident. Pores of various sizes are present, which are formed following the formation and release of volatile products through bubbles still visible at the surface (Fig. 2d). Further information can also be gained from the SEM images reported in Fig. 3a–b which refer to a charred residue obtained from a thermogravimetric test conducted in air at low temperature (5 K min^{-1} up to 750 K), when combustion rates are still negligible. The effects of material melting are again well evident with superficial burst bubbles that create some irregularity over an extremely smooth surface. The smoothness of the glossy surface and the absence of porosity are factors that play key roles for the scarce reactivity of this material in air, as shown in the following.

Contrary to the behavior of Divinycell and as already observed for wood pyrolysis [39, 40], the balsa char sample presents the same features as those of the original material but again with some shrinkage (about 15 % along the grain direction and 10 % along the perpendicular grain direction) and the appearance of small surface fissures, due to the internal overpressures during volatile species release [18, 41, 42] (Fig. 1b). Similar to the chars produced from both hardwood [35, 43] and softwood [44] varieties and in agreement with previous results [21], the balsa char preserves the main structural features of the virgin material, and the general morphological arrangement is not destroyed by the pyrolysis process. More precisely, the balsa wood structure is composed of larger diameter water transport vessels surrounded by a cellular network of tracheids and rays which, following pyrolysis, present a reduced wall thickness (Fig. 4a–b, grain cross section) (a detailed analysis about the structure of balsa wood and corresponding char is reported in [21]).

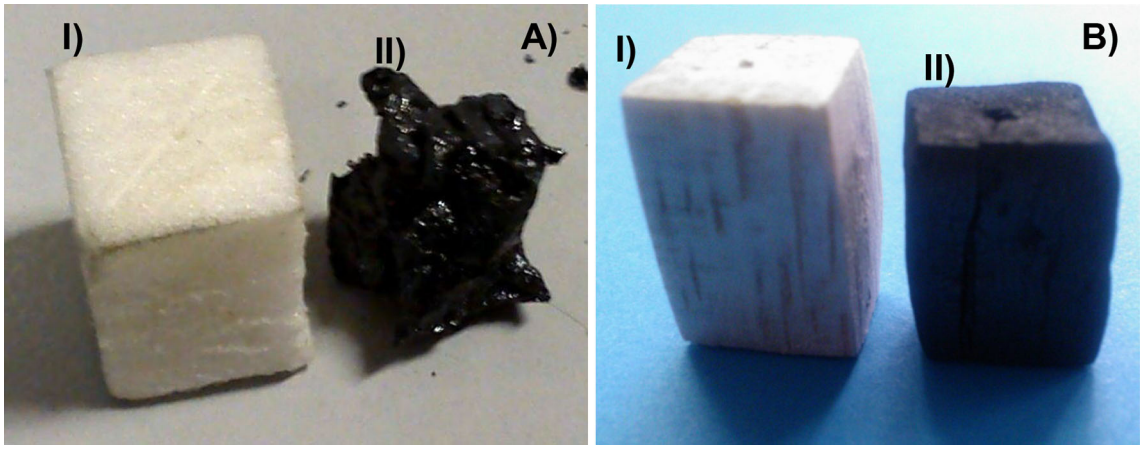

Fig. 1 Snapshots of the thick Divinycell sample (**a**) and the thick balsa wood sample (**b**) before (*I*) and after (*II*) pyrolysis at 950 K

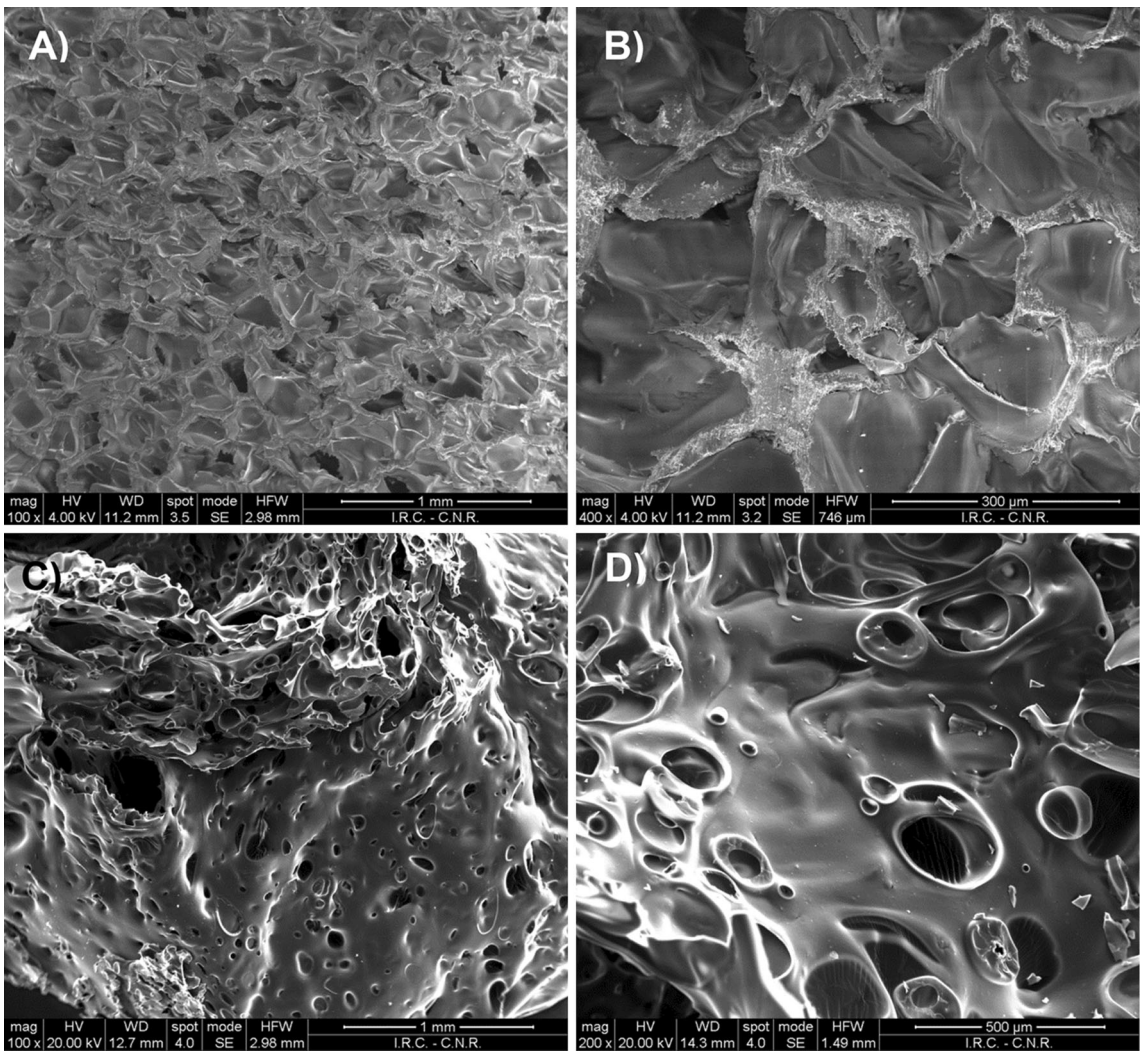

Fig. 2 SEM images of the cellular structure of Divinycell before pyrolysis (**a**, **b**) and surface morphology of the corresponding char produced from pyrolysis at 950 K (**c**, **d**)

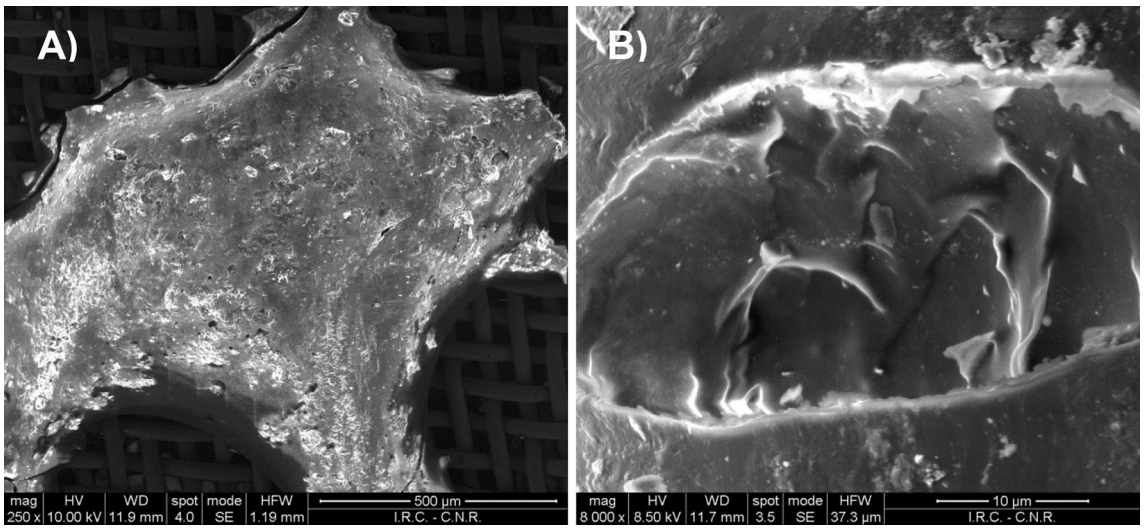

Fig. 3 SEM images of the surface morphology of char from Divinycell obtained by means of a thermogravimetric test in air at 5 K min^{-1} up to 750 K

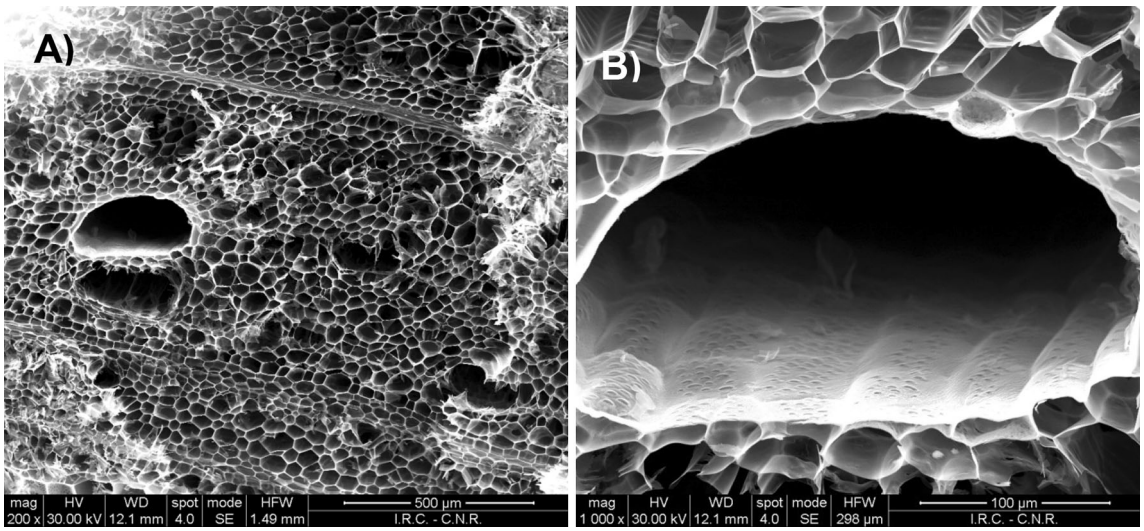

Fig. 4 SEM images of the char produced from balsa wood pyrolysis at 950 K (grain cross section)

Thermogravimetric behavior

Mass loss curves for the polymeric foam are measured at heating rates between 5 and 15 K min^{-1} up to a final temperature of 950 K. An example of the solid mass fraction and the corresponding first and second time derivative versus time (heating rate of 5 K min^{-1}) is displayed in Fig. 5. The second derivative of the solid mass fraction is used in the analysis of thermogravimetric data to define some characteristic points of the mass loss rate curves, specifically the initial and peak temperatures of shoulder zones (see, for instance, Refs. [45, 46]), useful for kinetic modeling. The beginning of the shoulder zone is associated with a characteristic temperature defined by extrapolating the slope of the devolatilization rate in correspondence with the first local maximum in $-d^2Y/dt^2$ (up to the zero level of the Y axis). Then, the decomposition temperature of this zone is defined by the point where $-d^2Y/dt^2$ attains the value nearest to zero in this region. Hence, apart from providing the main characteristics of the mass loss process, the curves can also be used to introduce the following parameters: initial degradation temperature, T_i, (the temperature corresponding to the release of 1 % of the total volatiles), characteristic temperatures, T_{pi}, (temperatures in correspondence of the peaks and shoulders of the mass release rate curve), corresponding mass fractions, Y_{pi}, rates of mass loss, dY_{pi}, and final degradation temperature, T_f, (the temperature corresponding to the release

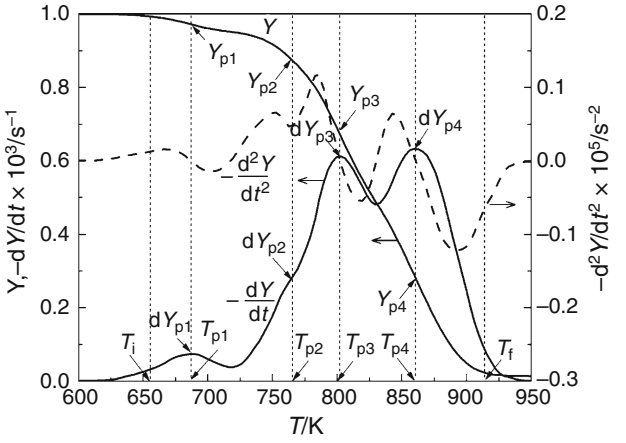

Fig. 5 Mass fraction, Y, and first and second time derivative, $-\mathrm{d}Y/\mathrm{d}t$ and $-\mathrm{d}^2Y/\mathrm{d}t^2$, for Divinycell in air versus time for a heating rate of 5 K min^{-1} up to 950 K with the definition of thermogravimetric parameters: initial degradation temperature, T_i, characteristic temperatures, T_{pi}, (temperatures in correspondence of the shoulders and peaks of the mass release rate curve), corresponding mass fractions, Y_{pi}, rates of mass loss, $\mathrm{d}Y_{pi}$, and final degradation temperature, T_f

Table 1 Characteristic parameters of the thermogravimetric curves measured in air for Divinycell at three heating rates, h: initial degradation temperature, T_i, temperatures, T_{pi}, at the shoulders and peaks of the mass release rate curve, corresponding mass fractions, Y_{pi}, rates of mass loss, $\mathrm{d}Y_{pi}$, and final degradation temperature, T_f

	h/K min^{-1}		
Parameters	5	10	15
T_i/K	663	676	680
T_{p1}/K	687	688	692
Y_{p1}	0.97	0.98	0.98
$-(\mathrm{d}Y/\mathrm{d}t)_{p1} \times 10^3$/s^{-1}	0.076	0.13	0.15
T_{p2}/K	765	766	770
Y_{p2}	0.88	0.91	0.92
$-(\mathrm{d}Y/\mathrm{d}t)_{p2} \times 10^3$/s^{-1}	0.28	0.34	0.51
T_{p3}/K	802	819	826
Y_{p3}	0.68	0.67	0.69
$-(\mathrm{d}Y/\mathrm{d}t)_{p3} \times 10^3$/s^{-1}	0.61	1.02	1.45
T_{p4}/K	861	855	896
Y_{p4}	0.28	0.25	0.26
$-(\mathrm{d}Y/\mathrm{d}t)_{p4} \times 10^3$/s^{-1}	0.64	1.32	1.89
T_f/K	916	932	947

of 99 % of volatile products). The values of these parameters are somewhat affected by the heating rate, as indicated in Table 1. In general, as observed in previous thermogravimetric studies [47], the onset of the various reaction stages is displaced at successively higher temperatures and the corresponding peak rates tend to increase, as the heating rate is augmented. For the material under study, the combustion process begins at temperatures around 650 K (T_i between 663 and 680 K) and is practically terminated for temperatures around 940 K (T_f between 916 and 947 K). The examination of the curves reported in Fig. 5 reveals the presence of a peak, a shoulder, and two further peaks, indicating that volatile products are released in accordance with at least a four-step process. The highest peak is observed at high temperatures (861–896 K, for the range of heating rates investigated), whereas the previous ones are positioned, in the order, at temperatures around 687–692, 765–770, and 802–826 K. Solid combustion generally occurs in two main stages representing oxidative degradation (devolatilization) of the original material and combustion of the char produced [19]. Hence, using the information gained from the pyrolysis experiments which establish that the yields of solid residue are around 42 %, it can be reasonably estimated that a temperature around 840 K demarks the devolatilization and combustion zones. Therefore, solid decomposition takes place according to three main steps, characterized by the release of relatively small amounts of volatiles, followed by a final reaction describing the combustion of char, which gives rise to the absolute peak rate and the production of the largest amount of volatiles. As already observed, the combustion behavior of Divinycell has never been studied, so a comparison with previous results cannot be made. However, it is interesting to observe that the devolatilization stage occurs according to three main zones, which are also observed and modeled for the thermal degradation of PVC [14, 15]. However, devolatilization of the material under study is displaced at significantly higher temperatures, most likely owing to specific properties of the main component and interactions with the other two components.

An interesting result for the combustion reactivity of the material is illustrated in Fig. 6 by means of a comparison between the mass loss characteristics as measured for the Divinycell sample and the char previously produced from the pyrolysis experiments (heating rate of 5 K min^{-1} up to 950 K). It is worth recalling that mass loss measurements for the polymeric foam are made using thin strips, whereas the char is oxidized in the form of a thin powdered layer. It appears that the mass loss begins approximately at the same temperature (possibly owing to the still significant volatile content of char), but the combustion peak is observed earlier (about 110 K) for the char (peak position at 750 vs 861 K). This behavior can be attributed to the extremely smooth surface and the absence of porosity of the char produced from the Divinycell strips, which are expected to result in a very small number of active carbon sites where oxygen adsorption onto the reaction surface and chemical reaction can actually occur [19]. The irregularities introduced by the milling process in the granular

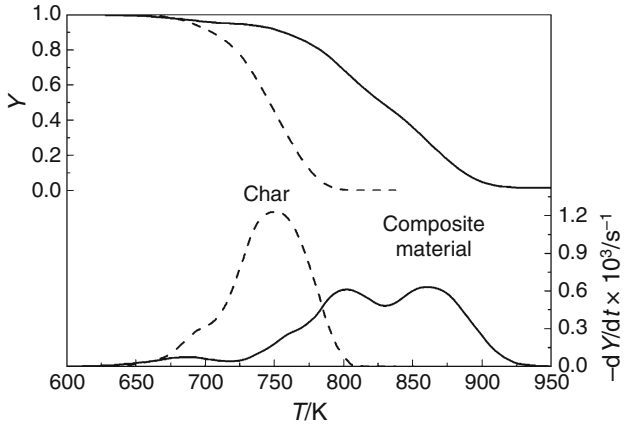

Fig. 6 Mass fraction, Y, and mass loss rate, $-\mathrm{d}Y/\mathrm{d}t$, for Divinycell and the corresponding char (produced from pyrolysis of a thick sample at 950 K) in air versus time for a heating rate of 5 K min^{-1} up to 950 K

char largely reduce these effects, and the surface area is certainly higher, thus explaining the increased reactivity. It can also be thought that the mass transfer limitations [48] play a more important role for the char produced from Divinycell strips.

The main thermogravimetric parameters for the balsa wood, as measured for heating rates between 5 and 20 K min^{-1}, are summarized in Table 2 (the definitions, which have the same meaning as in Fig. 5, can be seen in Fig. 7). In agreement with previous measurements made for different wood species and lignocellulosic fuels [19, 27, 34], combustion takes place in the temperature range of 475–740 K and various reaction zones appear corresponding to the devolatilization of the chemical components and the combustion of the resulting char. A shoulder (556–563 K), attributable to hemicellulose decomposition, is followed by the maximum peak (581–603 K), essentially associated with the release of volatile products from cellulose decomposition (lignin simultaneously degrades with the other two components), and finally, by another peak, representing char combustion (664–689 K). Again, the characteristic temperatures become progressively higher, as well as the corresponding devolatilization rates, as the heating rate is increased and compare well, from the quantitative point of view, with the results previously obtained for a hardwood species (beech) [27]. The sole difference is observed at low temperature where balsa wood shows slightly higher devolatilization rates, realistically due to a larger content of extractives, which are reported to play an important role in the shape of the mass loss rate curves [49]. Moreover, given the similar morphological and chemical properties of the char produced from the powdered wood sample used in thermogravimetry and the sample obtained from the pyrolysis experiments, no significant difference is

Table 2 Characteristic parameters of the thermogravimetric curves measured in air for balsa wood at three heating rates, h: initial degradation temperature, T_i, temperatures, T_{pi}, at the shoulders and peaks of the mass release rate curve, corresponding mass fractions, Y_{pi}, rates of mass loss, $\mathrm{d}Y_{pi}$, and final degradation temperature, T_f

	h/K min^{-1}		
Parameters	5	10	20
T_i/K	473	476	493
T_{p1}/K	556	560	563
Y_{p1}	0.71	0.74	0.81
$-(\mathrm{d}Y/\mathrm{d}t)_{p1} \times 10^3$/s^{-1}	0.74	1.22	1.77
T_{p2}/K	581	594	603
Y_{p2}	0.47	0.43	3.62
$-(\mathrm{d}Y/\mathrm{d}t)_{p2} \times 10^3$/s^{-1}	0.95	1.79	3.62
T_{p3}/K	664	677	689
Y_{p3}	0.11	0.12	0.13
$-(\mathrm{d}Y/\mathrm{d}t)_{p3} \times 10^3$/s^{-1}	0.23	0.44	0.94
T_f/K	713	727	740

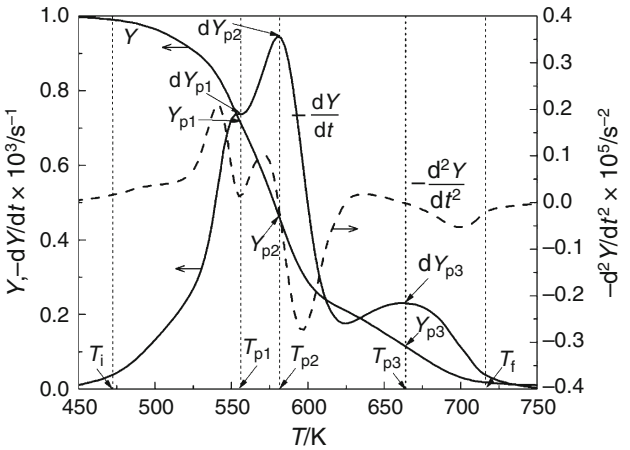

Fig. 7 Mass fraction, Y, and first and second time derivative, $-\mathrm{d}Y/\mathrm{d}t$ and $-\mathrm{d}^2Y/\mathrm{d}t^2$, for balsa wood in air versus time for a heating rate of 5 K min^{-1} up to 950 K with the definition of thermogravimetric parameters: initial degradation temperature, T_i, characteristic temperatures, T_{pi}, (temperatures in correspondence of the shoulders and peaks of the mass release rate curve), and corresponding mass fractions, Y_{pi}, and rates of mass loss, $\mathrm{d}Y_{pi}$, and final degradation temperature, T_f

observed in the temperature corresponding to the combustion peak (not shown).

An indication about the endothermic or exothermic nature of the various processes during the conversion for the two materials can be observed from Fig. 8 which reports the results of the differential thermal analysis. Apart from the effects of heat inertia [50] that are small, a wide endothermic zone, with a peak around 500 K is clearly observed for the Divinycell sample which can be

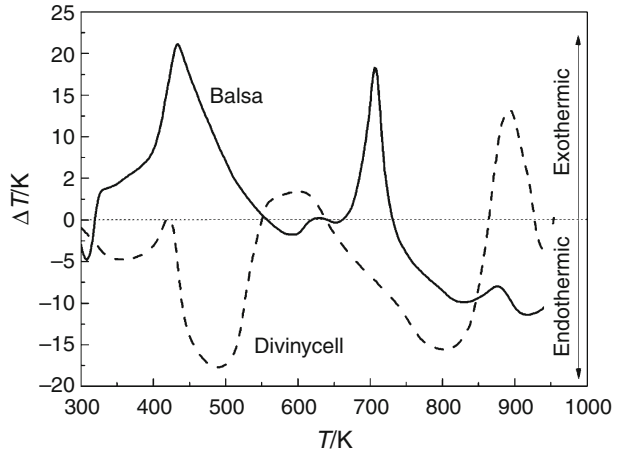

Fig. 8 Temperature difference between the sample and the empty sample holder for Divinycell and balsa wood, as obtained for an external heat flux profile recorded by requiring a heating rate of 15 K min^{-1} from ambient up to 950 K of the temperature of the empty sample holder

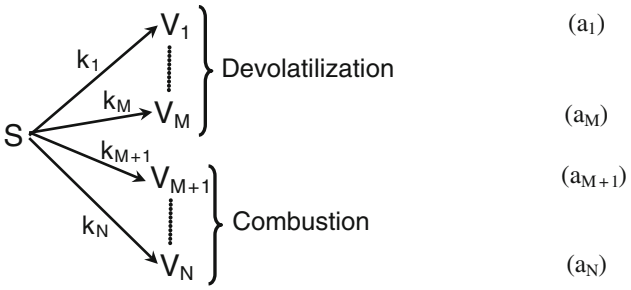

Fig. 9 Reaction scheme for the combustion of Divinycell and balsa wood

associated with the melting process well shown by the SEM images. No significant thermal event is observed for temperature around 550–650 K, as expected from the negligible mass loss rate (Fig. 5). Divinycell devolatilization (temperatures between 650 and 850 K) appears to be an endothermic process. Finally the combustion, at higher temperatures, of the charred residue occurs exothermally. The curve measured for balsa wood testifies that devolatilization at low temperature (350–500 K), essentially due to extractives and partly hemicellulose, is an exothermic process [51]. The devolatilization of the remaining fraction of wood (temperatures of 550–650 K) is barely endothermic, whereas the combustion of the charred residues is again an exothermic process.

Combustion kinetics

The analysis of the thermogravimetric curves for both core materials indicates that conversion in air occurs according to two main reaction stages, representing oxidative decomposition (of the material) and combustion of the resulting char. From the physical point of view, the two stages are sequential, but parallel reaction models are more flexible as they can easily guarantee this feature by an appropriate set of parameter values and, at the same time, can describe well the possible overlap between reactions [6, 7, 19, 27, 33, 34, 45, 46]. Then assuming that volatiles are released according to a set of parallel reactions for lumped components, the overall mass loss rate is a linear combination of the single component rates. Thus the kinetic model proposed for the samples of interest in this study consists of N independent parallel reactions as reported in Fig. 9, where S is the core material which produces the lumped volatile products V_i (i = 1,..,N). From the chemical point of view, reactions a_1,..,a_M are associated with solid devolatilization, and reactions a_{M+1},…,a_N are associated with char combustion. Based on the qualitative features shown by the thermogravimetric curves (Fig. 5; Table 1), it can be assumed that the combustion mode of Divinycell consists of three devolatilization reactions and one combustion reaction ($M = 3$ and $N = 4$). For balsa, the unified model recently developed [27] is proposed, extended to include the contribution of extractive degradation, and thus consisting of four devolatilization reactions (for the pseudo-components extractives, hemicellulose, cellulose, and lignin) and two char combustion reactions ($M = 4$ and $N = 6$) (the term "pseudo-component" is used as it is impossible in kinetic analysis to avoid overlap between different components in the measured mass loss curves [18]). The reactions rates present the usual Arrhenius dependence (A_i are the pre-exponential factors and E_i the activation energies) on the temperature and a power law dependence, exponent n_i, on the solid mass fraction. The latter treatment takes into account the evolution of the pore surface area during conversion [19]. Since the sample temperature, T, is a known function of time, the mathematical model consists of N ordinary differential equations for the mass fractions, Y_i, of the reacting solid fuel:

$$\frac{dY_i}{dt} = A_i \exp\left(-\frac{E_i}{RT}\right) Y_i^{ni}; \quad Y_i(0) = v_i, \quad i = 1, n \qquad (1-2)$$

In addition to the kinetic parameters (A_i, E_i, and n_i), the mass fractions of the lumped classes of volatiles generated, v_i, usually indicated as stoichiometric coefficients, are also estimated. The parameters are estimated through the numerical solution (implicit Euler method) of the mass conservation equations and the application of a direct method for the minimization of the objective function, which considers simultaneously both integral (TG) and differential (DTG) data for the various heating rates, thus avoiding possible compensation effects in the kinetic

Table 3 Estimated kinetic parameters (activation energy, E, pre-exponential factor, A, reaction order, n, and stoichiometric coefficient, v) for the combustion of Divinycell and corresponding deviations between measured and simulated integral (dev_{TG}) and differential (dev_{DTG}) curves (the parameters are invariant with the heating rate, h, except for small variations on the stoichiometric coefficients)

Parameters	h/K min^{-1}		
	3	5	7
E_1/kJ mol^{-1}	225.8		
A_1/s^{-1}	1.33×10^{15}		
n_1	1.10		
v_1	0.04	0.04	0.03
E_2/kJ mol^{-1}	261.0		
A_2/s^{-1}	4.14×10^{15}		
n_2	0.90		
v_2	0.03	0.03	0.03
E_3/kJ mol^{-1}	244.0		
A_3/s^{-1}	4.71×10^{13}		
n_3	1.20		
v_3	0.33	0.31	0.31
E_4/kJ mol^{-1}	220.0		
A_4/s^{-1}	5.82×10^{10}		
n_4	1.10		
v_4	0.59	0.61	0.62
%dev_{TG}	0.28	0.20	0.24
%dev_{DTG}	1.50	1.05	1.34

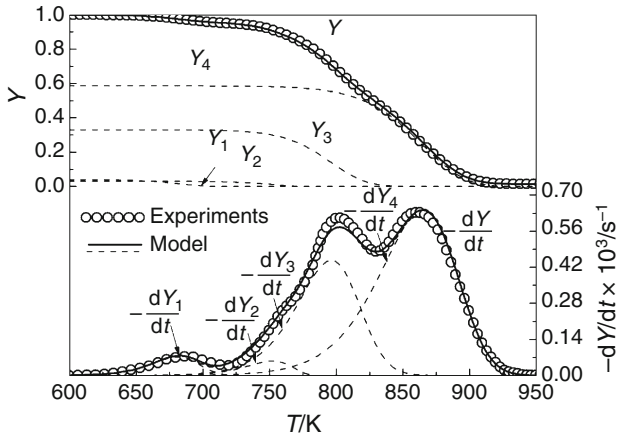

Fig. 10 Comparison between the measured (*symbols*) and the simulated (*solid lined*) mass fraction and rate of mass loss for Divinycell in air with heating rate, h, of 5 K min^{-1} up to 950 K. *Dashed lines* denote the predicted evolution of the mass fraction and rate of mass loss for the various reaction zones: 1,2,3 devolatilization of the composite material; 4 combustion of char (kinetic parameters listed in Table 3)

parameters [26], following the method already described [31]. The estimation procedure is implemented by requiring the same parameter values for all the measured curves,

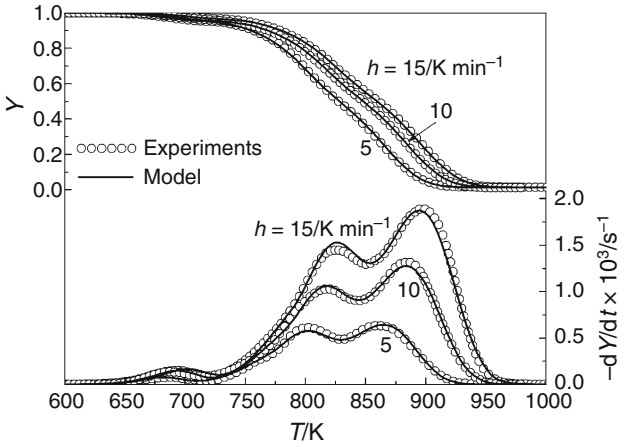

Fig. 11 Comparison between measured (*symbols*) and simulated (*solid lines*) thermogravimetric curves for Divinycell at various heating rates, h, in air up to a temperature 950 K (kinetic parameters listed in Table 3)

with the exceptions of the stoichiometric coefficients which are allowed to show small variations as a consequence of the dependence of the amounts of volatiles released during the first reaction stage on the heating rate. Finally, deviations between measurements and model predictions, dev_{TG} and dev_{DTG}, are defined as in [31].

The estimated values of the kinetic parameters and the deviations between predictions and measurements for the Divinycell sample are listed in Table 3. Figure 10 shows an example of the predicted dynamics of the single components and the comparison between measurements and predictions (heating rate of 5 K min^{-1}), whereas a comparison for the integral and differential data for all the heating conditions is shown in Fig. 11. The four-step kinetic model and the related parameters provide accurate predictions of the measured integral and differential curves in all cases. Moreover, it can be seen that the variations on the stoichiometric coefficients are small and average values can be used in practical applications. The three reactions for the devolatilization stage present rather high values of the activation energy (226, 261, and 244 Kj mol^{-1}) with amounts of released volatile products around 4, 3, and 32 %, respectively. For the combustion reaction, an activation energy of 220 kJ mol^{-1} is estimated, which is near to the upper limit typically reported for carbonaceous materials [19]. It is also worth observing that the amount of volatiles released in the combustion stage (around 60 %) is significantly higher than the amount of char measured in the pyrolysis experiments (42 %), due to the beginning of the combustion reaction at relatively low temperatures (around 750 K, see Fig. 10). Hence, as observed in the combustion of lignocellulosic chars, the actual combustion process is most likely preceded by char devolatilization.

Table 4 Estimated kinetic parameters (activation energy, E, pre-exponential factor, A, reaction order, n, and stoichiometric coefficient, ν) for the combustion of balsa wood and corresponding deviations between measured and simulated integral (dev_{TG}) and differential (dev_{DTG}) curves (the parameters are invariant with the heating rate, h, except for small variations on the stoichiometric coefficients). Data previously obtained for beech wood [27] are included for comparison

Parameters	Balsa			Beech		
	h/K min^{-1}					
	5	10	20	5	10	20
E_1/kJ mol^{-1}	113.7			–		
A_1/s^{-1}	2.69×10^9			–		
n_1	1.00			–		
ν_1	0.05	0.06	0.07	–		
E_2/kJ mol^{-1}	147.0					
A_2/s^{-1}	4.47×10^{11}			8.74×10^{11}		
n_2	1.00					
ν_2	0.26	0.24	0.22	0.22	0.23	0.24
E_3/kJ mol^{-1}	200.4					
A_3/s^{-1}	5.02×10^{15}					
n_3	1.00					
ν_3	0.34	0.34	0.36	0.40	41	0.41
E_4/kJ mol^{-1}	176.0					
A_4/s^{-1}	1.17×10^{13}					
n_4	1.00					
ν_4	0.08	0.09	0.09	0.09	0.09	0.09
E_5/kJ mol^{-1}	113.0					
A_5/s^{-1}	5.60×10^6					
n_5	1.00					
ν_5	0.11	0.11	0.11	0.13	0.11	0.11
E_6/kJ mol^{-1}	183.0					
A_6/s^{-1}	1.40×10^{12}			8.81×10^{11}		
n_6	1.45			1.54		
ν_6	0.15	0.15	0.14	0.15	0.15	0.14
%dev_{TG}	0.40	0.62	0.49	0.92	0.92	0.90
%dev_{DTG}	1.91	1.80	2.56	1.76	2.55	2.39

However, the kinetic analysis indicates that a further reaction step, describing this process, is not truly needed given that the application of a one-step reaction for the stage of char conversion produces small deviations between predictions and measurements in all cases. As expected, some overlap exists between the reaction zones. However, at low temperature (below 750 K) only two devolatilization reactions occur releasing small amounts of volatile matter, most likely including HCl. For temperatures in the range of 750–850 K, the third and most important devolatilization reaction takes place. The combustion of char, which is barely active in this temperature range, attains its maximum rate for temperatures around 850–950 K.

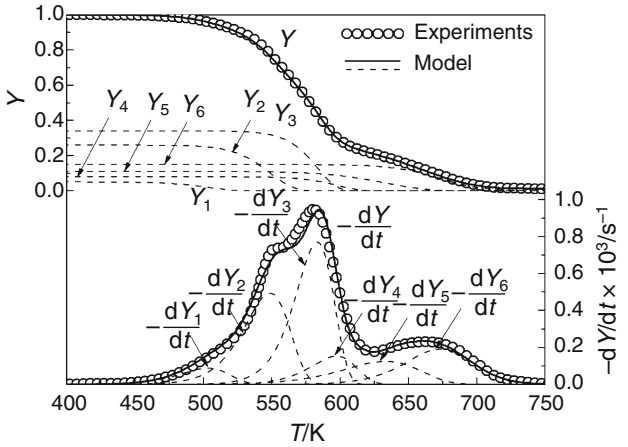

Fig. 12 Comparison between the measured (*symbols*) and the simulated (*solid lined*) mass fraction and rate of mass loss for balsa wood in air with heating rate, h, of 5 K min^{-1} up to 950 K. *Dashed lines* denote the predicted evolution of the mass fraction and rate of mass loss for the various reaction zones: 1,2,3,4 devolatilization, in the order, of pseudo-components extractives, hemicellulose, cellulose and lignin; 5,6 devolatilization and combustion of char (kinetic parameters listed in Table 4)

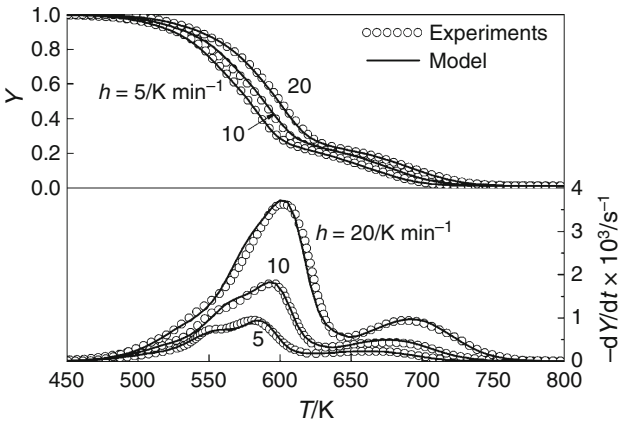

Fig. 13 Comparison between measured (*symbols*) and simulated (*solid lines*) thermogravimetric curves for balsa wood at various heating rates, h, in air up to a temperature 950 K (kinetic parameters listed in Table 4)

The estimated values of the kinetic parameters and the deviations between predictions and measurements for the balsa wood are listed in Table 4 where, for comparison purposes, the data previously estimated for beech wood [27] are also included. Figure 12 shows an example of the predicted dynamics of the single components and the comparison between measurements and predictions (heating rate of 5 K min^{-1}), whereas a comparison for the integral and differential data for all the heating conditions is shown in Fig. 13. The six-step kinetic model and the related parameters provide accurate predictions of the

measured integral and differential curves in all cases. The most important result is that, apart from the small contribution represented by the extractives (amounts of volatile released around 5 % and activation energy E_1 - = 114 kJ mol^{-1}), the activation energies for the devolatilization of pseudo-hemicellulose (E_2 = 147 kJ mol^{-1}), pseudo-cellulose (E_3 = 200.4 kJ mol^{-1}), and pseudo-lignin (E_4 = 176 kJ mol^{-1}) are the same as those already estimated for the devolatilization of beech wood in air [27]. Also, the activation energies for char devolatilization and combustion are the same (E_5 = 114 kJ mol^{-1}, E_6 - = 183 kJ mol^{-1}). In general, variations on the pre-exponential factors are also small, further supporting the concept that a unified model can be applied for the combustion of wood from the same classification. The main difference between balsa and beech wood concerns the percentages of volatiles produced from the decomposition of pseudo-components. These can possibly result from both different contents of the components and different amount and composition of ashes which, through catalysis, make more difficult mathematical separation between the various contributions [18].

Conclusions

The thermal behavior of two widely used core materials for sandwich structures (a PVC foam with the commercial name of Divinycell and balsa wood) has been investigated. Contrary to balsa wood which, when subjected to pyrolysis, preserve the main features of the original structural morphology, Divinycell undergoes partial melting and loses its cellular structure giving rise to a brittle non-porous and scarcely reactive char showing large superficial holes left by burst bubbles.

For both cases, thermogravimetric measurements in air show that the oxidative decomposition of the material is followed by the combustion of the resulting char. Oxidative decomposition, approximately occurring for temperatures between 650 and 940 K (Divinycell) and 475–740 K (balsa wood), is well described by three reactions and four reactions, respectively, with total volatile amounts of volatile products around 40 and 80 %. The stage of char combustion for an accurate description requires one (Divinycell) or two (balsa wood) reactions, although a char devolatilization stage is likely to exist also for the first material. A combustion model has for the first time developed for Divinycell, whereas a unified combustion model, previously presented by this research group for lignocellulosic materials, is shown to be also applicable for balsa wood with only small modifications in the pre-exponential factors and the introduction of a further step taking into account the degradation of extractives.

Acknowledgements This work is part of the activities carried out in the framework of the project COCET "Comportamento di Materiali Compositi in Condizioni Estreme: Alta Temperatura" (PON02_00029_3206086/F1), coordinated by IMAST and funded by the Italian Ministry of Instruction, University and Research (MIUR), the partial support of which is gratefully acknowledged. The authors also thank Mr. Luciano Cortese (Istituto di Ricerche sulla Combustione, CNR, Napoli, Italy) for the SEM images of the samples.

References

1. Mouritz AP, Gardiner CP. Compression properties of fire-damaged polymer sandwich composites. Compos Part A Appl Sci. 2002;33:609–20.
2. Looyeh MRE, Rados K, Bettess P. A one-dimensional finite element simulation for the fire-performance of GRP panels for offshore structures. Int J Numer Methods Heat Fluid Flow. 1997;7:609–25.
3. Galgano A, Di Blasi C, Branca C, Milella E. Thermal response to fire of a fibre reinforced sandwich panel: model formulation, selection of intrinsic properties and experimental validation. Polym Degrad Stab. 2009;94:1267–80.
4. Galgano A, Di Blasi C, Milella E. Sensitivity analysis of a predictive model for the fire behavior of a sandwich panel. Polym Degrad Stab. 2010;95:2430–44.
5. Marquis DM, Pavageau M, Guillaume E, Chivas-Joly C. Modelling decomposition and fire behaviour of small samples of a glass-fibre-reinforced polyester/balsa-cored sandwich material. Fire Mater. 2012;37:413–39.
6. Di Blasi C, Branca C, Galgano A, Moricone R, Milella E. Oxidation of a carbon/glass reinforced cyanate ester composite. Polym Degrad Stab. 2009;94:1962–71.
7. Di Blasi C, Branca C, Galgano A, Milella E. Thermal and kinetic characterization of a toughened epoxy resin reinforced with carbon fibres. Thermochim Acta. 2011;517:53–62.
8. Gdoutos EE, Daniel IM, Wang KA. Failure of cellular foams under multiaxial loading. Compos Part A Appl Sci. 2002;33:163–76.
9. Tagarielli VL, Deshpande VS, Fleck NA. The high strain rate response of PVC foams and end-grain balsa wood. Compos Part B- Eng. 2008;39:83–91.
10. Starnes WH. Structural and mechanistic aspects of the thermal degradation of poly(vinyl chloride). Prog Polym Sci. 2002;27:2133–70.
11. Marcilla A, Beltran M. Thermogravimetric kinetic study of poly (vinyl chloride) pyrolysis. Polym Degrad Stab. 1995;48:219–29.
12. Marcilla A, Beltran M. Kinetic models for the thermal decomposition of commercial PVC resins and plasticizers studied by thermogravimetric analysis. Polym Degrad Stab. 1996;53:251–60.
13. Beltran MI, Garcia JC, Marcilla A, Hidalgo M, Mijangos C. Thermal decomposition behaviour of crosslinked plasticized PVC. Polym Degrad Stab. 1999;65:65–73.
14. Miranda R, Yang J, Roy C, Vasile C. Vacuum pyrolysis of PVC I. Kinetic study. Polym Degrad Stab. 1999;64:127–44.
15. Anthony GM. Kinetic and chemical studies of polymer crosslinking using thermal gravimetry and hyphenated methods. Degradation of polyvinylchloride. Polym Degrad Stab. 1999;64:353–7.
16. Levchik SV, Weil ED. Overview of the recent literature on flame retardancy and smoke suppression in PVC. Polym Adv Technol. 2005;16:707–16.
17. Czegeny Z, Blazso M. Thermal decomposition of polyamides in the presence of poly(vinyl chloride). J Anal Appl Pyrolysis. 2001;58–59:95–104.

18. Di Blasi C. Modeling chemical and physical processes of wood and biomass pyrolysis. Prog Energy Combust Sci. 2008;34:47–90.
19. Di Blasi C. Combustion and gasification rates of lignocellulosic chars. Prog Energy Combust Sci. 2009;35:121–40.
20. Saito M, Amagai K, Ogiwara G, Arai M. Combustion characteristics of waste material containing high moisture. Fuel. 2001;80:1201–9.
21. Goodrich TW, Lattimer BY. Fire decomposition effects on sandwich composite materials. Compos Part A Appl Sci. 2012;43:803–13.
22. Lattimer BY, Ouellette J, Trelles J. Measuring properties for material decomposition modeling. Fire Mater. 2011;35:1–17.
23. Grenier AT, Dembsey NA, Barnett JR. Fire characteristics of cored composite materials for marine use. Fire Saf J. 1998;30:137–59.
24. Dembsey NA, Jacoby DJ. Evaluation of common ignition models for use with marine cored composites. Fire Mater. 2000;24:91–100.
25. Giancaspro J, Balaguru PN, Lyon RE. Use of inorganic polymer to improve the fire response of balsa sandwich structures. J Mater Civil Eng. 2006;18:390–7.
26. Conesa JA, Marcilla A, Caballero JA, Font R. Comments on the validity and utility of the different methods for kinetic analysis of thermogravimetric data. J Anal Appl Pyrolysis. 2001;58–59:617–33.
27. Branca C, Di Blasi C. A unified mechanism of the combustion reactions of lignocellulosic fuels. Thermochim Acta. 2013;565:58–64.
28. http://www.nfgsales.com/files/active/0/Divinycell_11-19-10.pdf.
29. Di Blasi C, Branca C, Galgano A. Biomass screening for the production of furfural via thermal decomposition. Ind Eng Chem Res. 2010;49:2658–71.
30. Lanzetta M, Di Blasi C, Buonanno F. An experimental investigation of heat transfer limitations in the flash pyrolysis of cellulose. Ind Eng Chem Res. 1997;36:542–52.
31. Branca C, Di Blasi C, Horacek H. Analysis of the combustion kinetics and the thermal behavior of an intumescent system. Ind Eng Chem Res. 2002;41:2104–14.
32. Branca C, Di Blasi C, Casu A, Morone V, Costa C. Reaction kinetics and morphological changes of a rigid polyurethane foam during combustion. Thermochim Acta. 2003;399:127–37.
33. Branca C, Di Blasi C. Devolatilization and combustion kinetics of wood chars. Energy Fuels. 2003;17:1609–15.
34. Branca C, Di Blasi C. Global intrinsic kinetics of wood oxidation. Fuel. 2004;83:81–7.
35. Branca C, Di Blasi C, Elefante R. Devolatilization and heterogeneous combustion of wood fast pyrolysis oils. Ind Eng Chem Res. 2005;44:799–810.
36. Branca C, Di Blasi C. Char structure and combustion kinetics of a phenolic-impregnated honeycomb material. Ind Eng Chem Res. 2013;52:14574–82.
37. Li X, Chen D. Synthesis and characterization of aromatic/aliphatic co-polyureas. J Appl Polym Sci. 2008;109:897–902.
38. Herrera M, Matuschek G, Kettrup A. Main products and kinetics of the thermal degradation of polyamides. Chemosphere. 2001;42:601–7.
39. Di Blasi C, Gonzalez Hernandez E, Santoro A. Radiative pyrolysis of single moist wood particles. Ind Eng Chem Res. 2000;39:873–82.
40. Di Blasi C, Branca C, Santoro A, Perez Bermudez RA. Weight loss dynamics of wood chips under fast radiative heating. J Anal Appl Pyrolysis. 2001;57:77–90.
41. Di Blasi C. Influences of model assumptions on the predictions of cellulose pyrolysis in the heat transfer controlled regime. Fuel. 1996;75:58–66.
42. Di Blasi C. Modelling intra- and extra-particle processes of wood fast pyrolysis. AIChE J. 2002;48:2386–97.
43. Branca C, Di Blasi C. Combustion kinetics of secondary biomass chars in the kinetic regime. Energy Fuels. 2010;24:5741–50.
44. Branca C, Di Blasi C. Oxidation characteristics of chars generated from wood impregnated with $(NH_4)_2HPO_4$ and $(NH_4)_2SO_4$. Thermochim Acta. 2007;456:120–7.
45. Gronli MG, Varhegyi G, Di Blasi C. Thermogravimetric analysis and devolatilization kinetics of wood. Ind Eng Chem Res. 2002;41:4201–8.
46. Varhegyi G, Gronli MG, Di Blasi C. Effects of sample origin, extraction and hot water washing on the devolatilization kinetics of chestnut wood. Ind Eng Chem Res. 2004;43:2356–67.
47. Branca C, Albano A, Di Blasi C. Critical evaluation of wood devolatilization mechanisms. Thermochim Acta. 2005;429:133–41.
48. Nowak B, Karlstrom O, Backman P, Brink A, Zevenhoven M, Voglsam S, Winter F, Hupa M. Mass transfer limitation in thermogravimetry of biomass gasification. J Therm Anal Calorim. 2013;111:183–92.
49. Sebio-Punal T, Naya S, Lopez-Beceiro J, Tarrio-Saavedra J, Artiaga R. Thermogravimetric analysis of wood, holocellulose, and lignin from five wood species. J Therm Anal Calorim. 2012;109:1163–7.
50. Sestak J, Holba P. Heat inertia and temperature gradient in the treatment of DTA peaks. Existing on every occasion of real measurements but until now omitted. J Therm Anal Calorim. 2013;113:1633–43.
51. Di Blasi C, Branca C, Masotta F, De Biase E. Experimental analysis of reaction heat effects during beech wood pyrolysis. Energy Fuels. 2013;27:2665–74.